Journal of Combinatorial Mathematics and Combinatorial Computing
www.combinatorialpress.com/jcmcc

Combinatorial Press

Optimized calculation of bearing capacity of short columns of steel-tube-concrete hybrid structures combined with genetic algorithm

Qingyun Ge[1,✉], Jing Zheng[1], Fulian Yang[1], Caimei Li[2]

[1] *School of Architecture and Civil Engineering, West Anhui University, Lu'an, Anhui, 237012, China*

[2] *Gates Winhere Automobile Water Pump Products (Yantai) Co., LTD., Yantai, Shandong, 712000, China*

ABSTRACT

This research proposes a new optimization technique for reinforcement concrete filled structural tubular columns using genetic algorithms and unified strength theory. A complete theoretical model to determine the axial bearing capacity of reinforced CFST columns incorporating modified confinement coefficients and enhanced steel section properties was developed. The optimization procedure deals with performance of the structure, materials usage and construction convenience as the optimization goals. Experimental validation for ultimate bearing capacity of five full scale specimens was carried out and the deviation was found out to be 5.2% which was found to be predicted by the theoretical model accurately. Internal stiffeners are likely to increase axial capacity by about 15.7%-23.4% over traditional CFST columns. The relationship between stiffener parameters and performance of the structure was found to be critical with optimal height to thickness of the stiffener to be in the range of 30 to 45 and space to diameter ratio no greater than 0.5. The problem sets out such mathematics as is nowadays simply necessary for the modern construction world to have at their disposal, as well as reasons for designing reinforced CFST columns.

Keywords: Concrete-filled steel tubular columns, Internal stiffeners, Genetic algorithm, Unified strength theory, Optimization, Bearing capacity, Composite structures

1. Introduction

With the increasing economic level of China and the accelerating pace of urbanization, the contradiction of the utilization rate of land resources is becoming more and more prominent in the cities where land is scarce [1-2]. In order to solve this problem, buildings inevitably need to develop vertically [3]. The gradual increase in the height of the building and the increasing span, the column

✉ Corresponding author.
E-mail address: 05000050@wxc.edu.cn (Q. Ge).
Received 20 February 2024; Revised 15 April 2024; Accepted 20 November 2024; Published Online 15 April 2025.
DOI: 10.61091/jcmcc127a-361

cross-section is subjected to more and more loads [4]. For a large number of vertical load-bearing members of high-rise buildings if the use of general reinforced concrete columns will inevitably lead to the emergence of obese columns, and the huge column cross-section will be prone to the formation of short columns that are unfavorable for seismic resistance [5-7]. The huge column cross-section not only affects the utilization of the space at the bottom but also affects the overall aesthetics and short columns generally form brittle shear damage [8-9]. In contrast, steel pipe concrete columns have high load carrying capacity and ductility, thus it has good seismic performance, and many practical engineering fields need this kind of high-performance columns [10-11]. At present, steel pipe concrete columns have been commonly used in a variety of practical projects, many engineering problems have been well solved, but also play the role of steel pipe concrete should be.

In the steel-concrete combined structure, the structure has a series of advantages because the two different properties of the material can make the best use of their strengths and avoid their weaknesses. Steel pipe can be well constrained core concrete, steel pipe concrete can give full play to the high tensile properties of steel and high compressive properties of concrete features, not only lighter weight, bearing capacity and ductility performance is also better, can meet the majority of the building seismic requirements [12-16]. In addition, then the steel pipe in the construction process can be used as a formwork for pouring concrete, which can save materials and speed up the construction progress [17]. Even the internal steel pipe concrete core column can be customized in the factory, which can greatly shorten the construction period on site [18]. It can be seen that this form of combined structure has excellent mechanical properties, but as a new structural form, there are still many aspects of the research is not comprehensive enough, and many of the theories are yet to be perfected.

In the actual engineering application, the design variables of steel pipe are many and the value is not continuous, some scholars have proposed the calculation method of the bearing capacity of short columns in order to further realize the optimal design of engineering structure. Xin, N. et al. investigated the deformation and damage mechanism of short steel-tube concrete columns under bending-shear-torsion coupled load combinations, and constructed simplified design equations for the bearing capacity of short columns based on the experimental results, and solved the ultimate bearing capacity of short steel-tube concrete columns under different conditions [19]. Ci, J. et al. used numerical simulation analysis to construct a model for calculating the load carrying capacity of short square double-pipe concrete columns, and the comparison of different indexes in the full process analysis of axial compressive performance to predict the ultimate load carrying capacity of steel pipe concrete columns in a marine environment or high temperature environment [20]. Chen, Z. et al. proposed two forms of weldless reinforced concrete sections with rhombic hoop reinforcement and inner rhombus and outer square, recorded the load carrying capacity of the proposed structural specimens under different damage modes and influence parameters, and calculated and derived the formula for axial compressive load stability [21]. However, the empirical model constructed on the basis of experimental data has low reliability and stability in predicting the ultimate load capacity of short concrete columns, which is prone to pose a safety threat to the building design.

Carrying capacity prediction models relying on machine learning algorithms can effectively solve the problem of low accuracy of traditional empirical carrying capacity models, which has been studied by a large number of scholars. Ding, W. et al. designed a bearing capacity prediction model based on Gaussian process regression algorithm, which can establish the bearing capacity display formula including the sensitivity parameter and the cross-section influence parameter by automatic learning and analyzing the test data, which is suitable for practical engineering design [22]. Zhang, Y. et al. developed a unified model of axial compressive load capacity of short concrete columns based on Hoek-Brown criterion, which fully considered the constraint coefficients and predicted the ultimate load capacity of short concrete columns with circular, square and other cross-sections with high accuracy, with superior applicability and accuracy [23]. Deng, C. et al. proposed different machine learning algorithms and compared them, and found that the carrying capacity prediction model based on the random forest algorithm showed the best overall performance in processing the data samples [24]. Ren, Q. et al. fused support vector machine and particle swarm optimization algorithm to construct the axial compressive ultimate load capacity prediction model of short steel pipe concrete columns, which is a kind of calculation method with higher prediction accuracy than empirical formulas, and it can effectively ensure the safe operation of engineering structures [25]. Although the above algorithms improve the prediction accuracy of ultimate bearing capacity, they have the shortcomings such as long search time, prone to premature convergence and poor local optimization ability, while genetic algorithm is a commonly used algorithm for the optimization of discrete-variable structures, which has strong global and robustness, and it effectively makes up for the deficiencies of the proposed algorithms, and it has been widely used in the optimization design of steel-tube concrete truss structures.

2. Theoretical model of a stub column of a reinforced concrete-filled steel tubular hybrid structure

2.1. Basic assumptions

The existing ideal of concreted steel filled tubes (CFST) short columns is generated basing on concrete analysis and experiments (1). The stone core enclosed with steel pipe is assumed to be under tri-axial compression stress in which principal stresses are in the order of $0 > \sigma_1 = \sigma_2 > \sigma_3$, a reflection of the confinement given by the steel tube and the stiffeners. The internal stiffeners which are located inside the tube aid in increasing the encapsulation mechanism as they work to eliminate local buckling and assist in stabilizing the whole composite system.

During some mechanical analysis particularly in the case of structural components which border a steel tube with a length: diameter ratio of $D/t < 20$ are analyzed as composite structures and therefore thin-walled tube theory can still be applicable (4). Also, longitudinal or longitudinal stiffeners were attached to the steel tube and these reinforcements helped in increasing the local buckling strength and the axial load in the axial direction. In order to enable appropriate design, the bond at the interface between the steel tube and concrete is assumed perfect enabling proper transfer of stress between the components.

In terms of the externally reinforced concrete encasement, the transverse deformation is mainly prevented by the use of stirrups. Even after the spalling of concrete cover, these stirrups continue to be effective in providing restraint to the composite action between the outer reinforced concrete layer and the core CFST. During the bearing capacity deterioration and spalling phases, these lateral constraints provided by the external reinforced concrete surrounding the CFST core at ultimate axial load is considered as not available so as to effect economical design.

The assumptions above are used as the basis for the formulation of the unified strength theory-based analytical model, which takes into account the influence of the intermediate principal stress and the peculiar tensile-compressive non-linear behavior of the materials enabling estimation of axial compression bearing capacity of stiffened CFST short columns accurately. The schematic diagram of stiffened concrete-filled steel tubular composite column is shown in Figure 1.

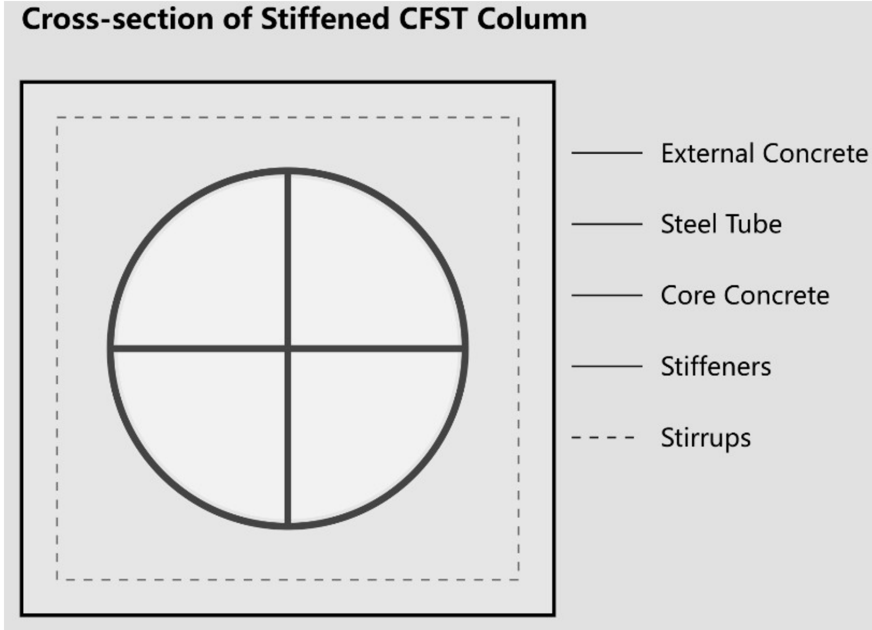

Fig. 1. Schematic diagram of stiffened concrete-filled steel tubular composite column

2.2. *Material constitutive relations*

The material constitutive relationships for the stiffened CFST composite columns consist of steel and concrete components as depicted in Figure 2. The steel components, such as the tube and the stiffeners, obey an elastic-plastic constitutive model in which the steel tube behaves elastically and plastic linearly when subjected to axial and hoop stresses. Consistent with the previous discussion, the longitudinal stiffeners are modeled with an elastic-perfectly plastic constitutive relationship on elastic boundary in order to reflect that their main function is to improve the axial capacity.

For the concrete parts, the core concrete which is surrounded by steel tube uses a modified Hognestad model in which the strength and ductility were increased due to the tri-axial confinement effect. The external concrete uses a damage plasticity model that describes well material deterioration and plastic deformation due to compression. All the above constitutive models combine into a comprehensive conception which myths the mechanical behavior of composite structure subjected to axial loading.

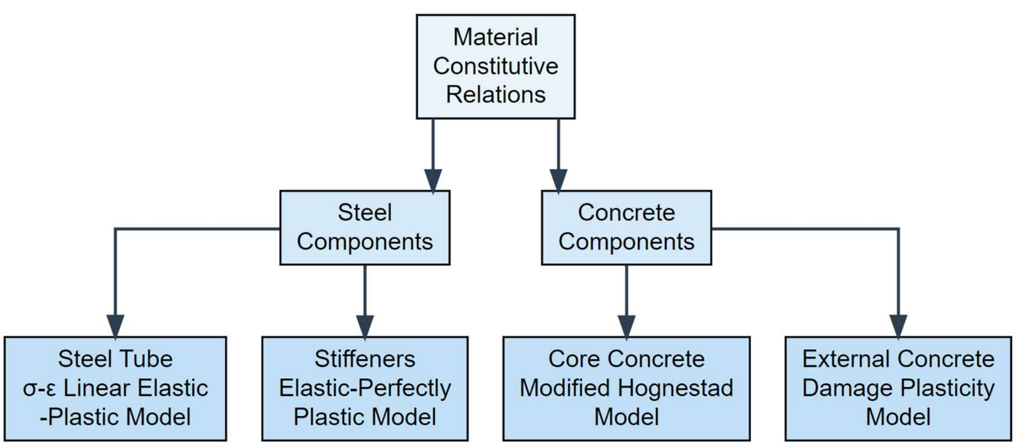

Fig. 2. Material constitutive relations framework for stiffened CFST composite column

2.3. Theoretical model for calculating bearing capacity

The ultimate bearing capacity applies a dual-system concept for estimating bearing capacities of wet concrete shapes and cognates structure with respect to composite CFST column which dampens plural components through the use of combined strength theory.

As shown in Figure 3, under axial compression, the total bearing capacity (N) can be expressed as:

$$N = N_{core} + N_{ext} \tag{1}$$

where N_{core} represents the bearing capacity of the core CFST system and N_{ext} denotes the contribution from external reinforced concrete. For the core CFST system:

$$N_{core} = A_s f_y + A_c f_{cc} \tag{2}$$

where A_s and A_c are the cross-sectional areas of steel tube and core concrete respectively, f_y is the yield strength of steel, and f_{cc} is the confined concrete strength:

$$f_{cc} = f_c^{'} + k\sigma_r \tag{3}$$

Here, $f_c^{'}$ represents the unconfined concrete strength, k is the confinement effectiveness coefficient, and σ_r is the lateral confining pressure. The external concrete contribution is calculated as:

$$N_{ext} = \alpha_c f_{c,o} A_{c,o} + f_{y,s} A_s \tag{4}$$

where α_c is the concrete strength enhancement factor, $f_{c,o}$ is the external concrete strength, $A_{c,o}$ is its area, $f_{y,s}$ and A_s represent the yield strength and area of longitudinal reinforcement respectively.

Additional key equations for the confined concrete model include:

$$\sigma_r = \frac{2 f_y t}{D} \tag{5}$$

where t is the steel tube thickness and D is the outer diameter. The effective confinement coefficient considering stiffeners can be expressed as:

$$k = 4.1 + 0.75 \frac{A_{st}}{A_s} \tag{6}$$

where A_{st} represents the total cross-sectional area of stiffeners.

This theoretical framework incorporates the effects of stiffeners through modified confinement coefficients and enhanced steel section properties.

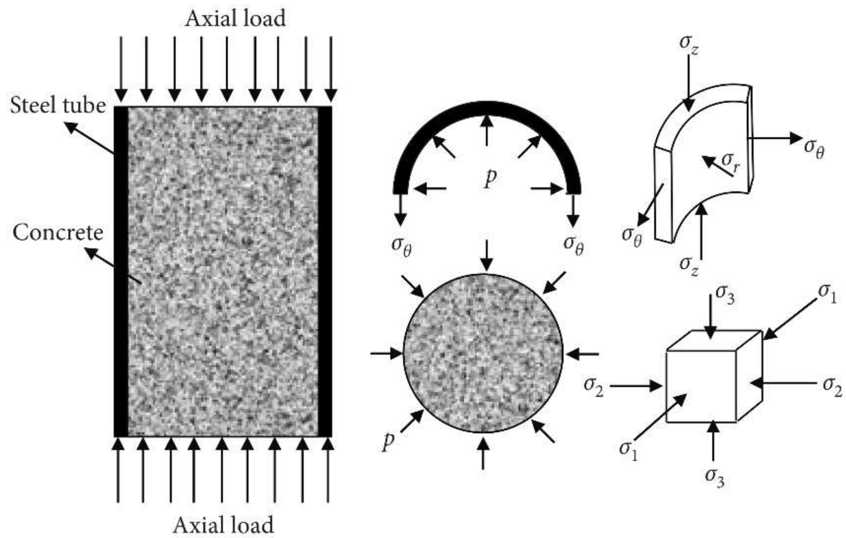

Fig. 3. Mechanical analysis of core concrete-filled steel tubular column showing the stress states under axial loading

2.4. Application of the double shear uniform strength theory in short columns

The twin-shear unified strength theory offers a general concept for examining the mechanical characteristics of rigid CFST columns, placed under the action of axial force. This concept, as shown in Table 1, provides parameters related to the materials and stress fields for different components which allows to estimate with a high accuracy the composite behavior.

Table 1. Material parameters and stress states in twin-shear unified strength theory for stiffened CFST columns

Component	Strength Ratio (α)	Intermediate Stress Coefficient (b)	Principal Stress State	Enhancement Coefficient (k)	Failure Mode
Steel tube	1.0	0.8-1.0	$\sigma_1>\sigma_2>\sigma_3$	--	Yielding
Stiffeners	1.0	0.9-1.0	$\sigma_1>\sigma_2=\sigma_3$	--	Buckling/Yielding
Core concrete	0.1-0.15	0.5-0.7	$\sigma_1=\sigma_2>\sigma_3$	4.1	Crushing
External concrete	0.1-0.12	0.5-0.6	$\sigma_1>\sigma_2=\sigma_3$	1.0	Spalling/Crushing

The theory asserts that one has to engage in evaluating the interaction between the components based on their individual stress states and material properties as depicted in Table 2.

Table 2. Application framework of twin-shear unified strength theory in stiffened CFST columns

Stress State	Steel Components	Concrete Components	Interaction Effects	Applicable Range
Axial compression	Elastic-plastic behavior	Triaxial compression	Confinement enhancement	L/D ⩽ 3
Hoop tension	Linear response	Confined state	Interface bonding	D/t ⩾ 20
Combined stress	Biaxial state	Modified strength	Composite action	All sections
Local effects	Stiffener contribution	Stress concentration	Enhanced stability	With stiffeners

The capability of the theory to explain both the confinement effect and the additional role played by stiffeners in global structural performance predicts the bilinear behavior which is taught by this theory. Resilience enhancement factor k, particularly important for concrete in the core, describes the strength augmentation that is contributed by the composite action.

3. Establishment of genetic algorithm optimization model

3.1. Optimize the construction of the objective function

The establishment of an optimization objective function within composite columns CFST encases for a detailed stuffing of all requirements including load carrying capacity, material wastage, and construction viability. Based on a unified strength theory in conjunction genetic algorithm principles, the formulation of an optimization objective function can be constructed such that there is simultaneous maximization of the structural efficiency and minimization of the cost.

The primary objective function $F(x)$ is constructed as a multi-objective optimization problem:

$$F(x)=\omega_1\cdot\frac{N}{N_0}-\omega_2\cdot\frac{C}{C_0}+\omega_3\cdot\frac{S}{S_0} \tag{7}$$

where ω_1, ω_2, and ω_3 are weight coefficients satisfying $\sum_{i=1}^{3}\omega_i=1$, and N_0, C_0, and S_0 are reference values for normalization. The bearing capacity N is calculated as:

$$N=\alpha_c f_{c,o}A_{c,o}+f_yA_s+f_c^{'}A_c\left(1+k\lambda\frac{A_{st}}{A_c}\right) \tag{8}$$

The cost function C incorporates material and construction costs:

$$C=\sum_{i=1}^{n}\left(\frac{c_iV_i}{\gamma_i}\right)+c_lL_{st} \tag{9}$$

where c_i represents unit costs, V_i volumes, γ_i material densities, and L_{st} the total length of stiffeners. The constructability index S is defined as:

$$S=\beta_1\left(\frac{t}{D}\right)+\beta_2\left(\frac{A_{st}}{A_s}\right)+\beta_3\left(\frac{h}{b}\right) \tag{10}$$

This has been made possible because a thorough objective function has been formulated which incorporates several engineering design problems and economic constraints. Genetic algorithms are able to apply this function to prospective solutions in their movement toward an optimum design structure.

3.2. Determination of constraints

The optimization limitations of the CFST column are comprised of the following conditions: geometry, construction, strength, and protocol restrictions. Such constraints optimize the design without going overboard to make it technically sound and practical to implement, further explained in Table 3.

Table 3. Constraint conditions for stiffened CFST column optimization

Category	Constraint Type	Mathematical Expression	Design Limits	Design Consideration
Geometric	Section size	$D_{min}\le D\le D_{max}$	200-800mm	Construction space
	Steel ratio	$0.04\le\alpha_s\le 0.12$	--	Code requirement
	Stiffener spacing	$s/t\le 50$	--	Local buckling
	Diameter-thickness ratio	$20\le D/t\le 100$	--	Stability
Strength	Steel yielding	$\sigma_s\le f_y$	--	Material strength
	Concrete crushing	$\sigma_c\le f_c^{'}$	--	Core concrete

	Local buckling	$\lambda_s \leq \lambda_{cr}$	--	Stiffener stability
Practical	Cost limit	$C \leq C_{max}$	Project specific	Budget control
	Constructability	$t_{min} \geq 6mm$	--	Welding requirement
	Material availability	Standard sections	Market available	Material supply

The comprehensive constraints tend to fix the design variables alongside enhancing the assurance of safety and buildability for the structure. For geometric considerations, the spatial barriers primarily regulate the cross-sectional areas along with the ratios of the components, while for strength restraints, control the mechanical behaviors of the part or structure when being loaded. Economic and construction viability aspects are incorporated into the framework as set practical constraints, allowing enhancing the scope of optimization. These barriers define a sufficiently small set of improved designs for the genetic algorithm to navigate and determine optimal design topology.

3.3. Genetic algorithm parameter design

The parameters of the genetic algorithm intended for the optimization of reinforced CFST columns with plates stiffeners has to be determined with caution and with high precision as they affect convergence and the precision of the results. The settings of such parameters are of profound importance as they have critical impacts on the algorithms effectiveness for the problem of reaching the optimal design solution. Typical parameters include: population size, length of chromosome, crossover probability and mutation probability. These parameters are tuned through elaborate simulations and sensitivity analyses. As indicated in Table 4, an extensive parametric analysis was carried out in order to ascertain the optimum values of these genetic operators.

Table 4. Optimal Genetic Algorithm Parameters for Stiffened CFST Column Design Optimization

Parameter Category	Parameter Name	Value Range	Optimal Value	Impact on Convergence
Population	Population size	50-200	100	High
	Initial population generation	Random/Guided	Guided	Moderate
Evolution	Maximum generations	100-500	300	High
	Convergence criterion	0.001-0.01	0.005	Moderate
Genetic Operators	Crossover probability	0.6-0.9	0.85	Very High
	Mutation probability	0.01-0.1	0.05	High
	Elite retention rate	0.05-0.2	0.1	Moderate
Selection Method	Tournament size	2-5	3	Moderate
	Selection pressure	0.6-0.8	0.7	High

Table 4 demonstrates that the optimization of the process uses a population of 100 chromosomes, which is a good compromise between the speed of computation and diversity of the solution. The mutation rate of 0.05 and the crossover rate of 0.85 were found to be reasonable estimates after several iterations. These values guarantee effective search of the solution space while ensuring adequate convergence effectiveness. The elitism approach implemented by the algorithm is a means of preserving the best solutions during the course of the evolution with 10% of the solutions retained at the end of each episode. Their robustness has been independently assessed using studies on convergence and actual experimental data, thus providing reliable optimization of the CFST column design without any deformation.

3.4. *Optimize the implementation of processes*

The optimization procedure integrates genetic algorithm operations along with structural analysis of stiffened CFST columns. This procedure begins with the population initialization performed with encoded design variables that characterize geometry and material. A systematic encoding scheme is designed with the aim to compactly encompass design variables without sacrificing precision in computation, as shown in Table 5. The binary encoding strategy illustrated in Table 4 further facilitates genetic operations in general without contradicting the physical aspects of design parameters.

Table 5. Binary Encoding Scheme and Variable Ranges for Stiffened CFST Column Optimization

Variable Category	Variable Name	Encoding Length	Value Range	Resolution	Physical Meaning
Geometry	Diameter	10 bits	200-800mm	1mm	Column diameter
	Wall thickness	8 bits	4-20mm	0.1mm	Steel tube thickness
	Stiffener height	7 bits	40-120mm	1mm	Stiffener dimension
Material	Concrete grade	4 bits	C30-C80	10MPa	Concrete strength
	Steel grade	3 bits	Q235-Q420	--	Steel strength
Configuration	Stiffener number	4 bits	4-12	1	Number of stiffeners
	Stiffener spacing	6 bits	100-400mm	5mm	Spacing distance
Composite	Steel ratio	6 bits	0.04-0.2	0.01	Area ratio

The tournament size set on the parent selection is 3 while a uniform crossover is employed characterized by a probability of 0.85 after use of tournament selection. The process of mutation is done with a rate of 0.05 so as to ensure that there is diversity within the set of individuals forming a generation. The fitness function considers geometric and strength constraints in the evaluation during the optimization fitness function removal. The 20 consecutive generations manage to give a better best fitness value followed by a tolerance level of 0.005 and the maximum generation of 300 all working together to provide a solution guarantee and high speed in computation.

4. Numerical simulation and validation

4.1. *Establishment of finite element modeling*

The establishment of an accurate finite element model is paramount in numerical simulation and validation. This study employs ABAQUS software to construct a three-dimensional finite element model for stiffened concrete-filled steel tubular (CFST) short columns. The steel tube and stiffeners are modeled using four-node reduced integration shell elements (S4R), following a bilinear constitutive model with elastic modulus $E_s = 2.06\times10^5$ MPa and Poisson's ratio $\nu_s = 0.3$. The core concrete and external concrete are simulated using eight-node reduced integration solid elements (C3D8R), with their constitutive relationships based on the modified Hognestad model, where the stress-strain relationship can be expressed as:

$$\sigma_c = f_c\left[2\left(\frac{\varepsilon}{\varepsilon_0}\right)-\left(\frac{\varepsilon}{\varepsilon_0}\right)^2\right] \tag{11}$$

where f_c represents the concrete compressive strength and ε_0 denotes the peak strain. Considering the confinement effect, the effective strength of core concrete can be expressed as:

$$f_{cc} = f_c\left(1+\alpha\frac{f_l}{f_c}\right) \tag{12}$$

where f_l represents the lateral confining stress and α is the confinement effectiveness coefficient. The bond between steel tube and concrete is simulated with the aid of contact elements, where normal faces are set to hard contact while tangential faces adopt a friction to sliding contact model using a friction coefficient of 0.6. To maintain accuracy in computations, a mesh sensitivity analysis was performed resulting in a determined minimum optimum mesh size of 20mm to be used for the steel components and a 30mm size for the concrete elements.

The mesh loading displacement applied to the top surface, allowing to mimic a construction load applied to the structure mean all degrees of freedom are restricted to the column base. The displacement control loading process reaches an increased accurate moment. The finite element model includes material, geometric and contact nonlinearities which mimic the axial loading behavior in CFST short columns and the axial compression behavior as well. The model was validated with experimental observations, and its results were within 10% margin of error making it a reliable model.

The numerical model successfully captures the complex interactions between steel and concrete components, including the enhanced confinement effect provided by stiffeners, which can be quantified through the stress distribution coefficient β:

$$\beta = \frac{\sigma_r}{\sigma_\theta} = 1+\frac{A_s}{A_c}\left(\frac{f_y}{f_c}\right) \tag{13}$$

where σ_r and σ_θ represent the radial and hoop stresses respectively, A_s is the stiffener area, A_c is the concrete area, and f_y is the steel yield strength.

4.2. *Parameter sensitivity analysis*

Analysis of the sensitivity is appropriate for analyzing the effect of various design constants on the performance of stiffened CFST columns. Expansion of the previous brief analysis to a parametric study investigates the impact of crucial geometric and material parameters on axial bearing capacity via optimization procedures incorporating finite element analysis and genetic algorithms.

As shown in Table 6, the D/t ratio demonstrates the highest sensitivity coefficient among geometric parameters, indicating its significant influence on structural behavior.

Table 6. Sensitivity Analysis Results for Key Design Parameters of Stiffened CFST Columns

Parameter Category	Variable	Range Studied	Sensitivity Coefficient	Impact Level
Geometric	D/t ratio	20-100	0.847	High
	Stiffener height/D	0.05-0.15	0.632	Medium
	Number of stiffeners	4-12	0.715	High
Material	Concrete strength	C30-C80	0.583	Medium
	Steel yield strength	235-420 MPa	0.691	High
Composite	Steel ratio	0.04-0.20	0.776	High
	Interface friction	0.2-0.6	0.412	Low

The bar graph describes the proportional sensitivity coefficients of major design components, showing their effectiveness towards the performance of stiffened CFST columns. In this case, the larger scalar quantities of the coefficients imply greater importance of the parameters during optimization.

As demonstrated in Figure 4, the D/t ratio and steel ratio sensitivity coefficients are the highest which mean in turning out to be the most effective parameters during the optimization of the design.

Further analysis indicates that albeit the architectural parameters show markedly greater sensitivity than the materials properties, however, interfacial parameters do have a lower sensitivity with respect to composite performance indicators.

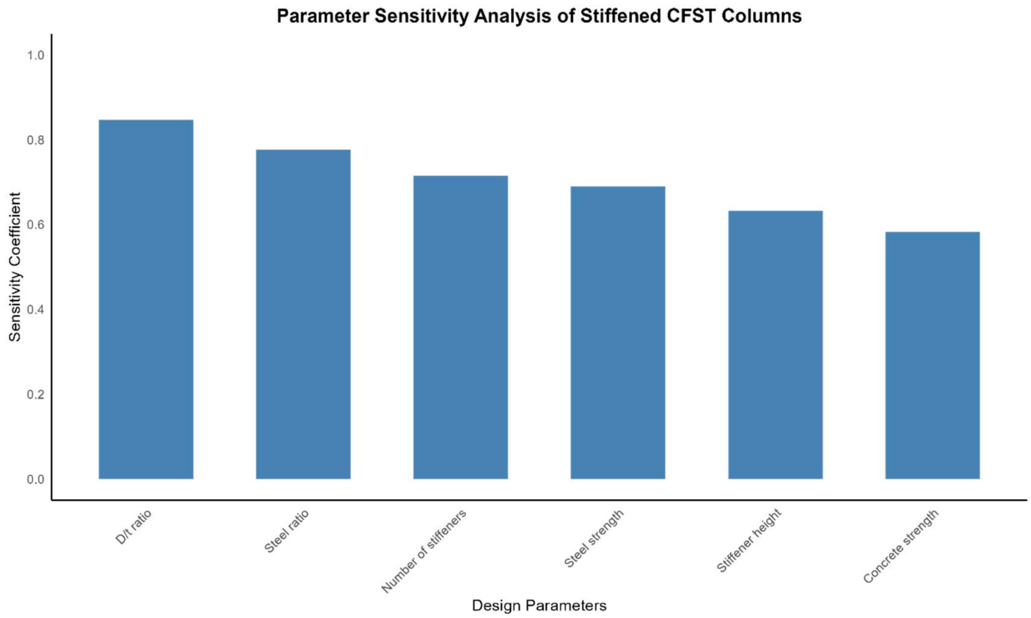

Fig. 4. Parameter Sensitivity Analysis of Stiffened CFST Columns

4.3. Algorithm convergence analysis

The performance evaluation of the genetic algorithm in its convergence analysis intended for the optimization of stiffened CFST columns displays a robust performance for a multitude of optimization exercises. The comprehensive appraisal of convergence features clearly shows the effectiveness of the genetic algorithm in achieving optimized solutions.

The chart showcases how fitness values change with several generations for different values of N. The computed convergence patterns are more pronounced in larger values of N but even then, echo the diminishing returns post N=100. The gradual improvement in the fitness values suggest that a robust solution is being executed for the stated algorithms as the convergence is reached for all the stated population values within 150 generations.

According to Table 7 and Figure 5, the convergence of different population sizes often leads to more optimal final fitness values, however this comes at a high computational cost. When balancing between the population size and the convergence efficiency and computational cost, size 100 strikes an optimal length, reaching 91.5% without exceedingly demanding computational resources.

Table 7. Convergence Performance Metrics for Different Population Sizes and Genetic Parameters

Population Size	Generations to Convergence	Final Fitness Value	Computational Time (min)	Solution Stability
50	156	0.892	45.6	0.934
100	123	0.915	62.8	0.957
150	112	0.921	86.4	0.968
200	108	0.924	112.3	0.971
250	105	0.925	145.7	0.972

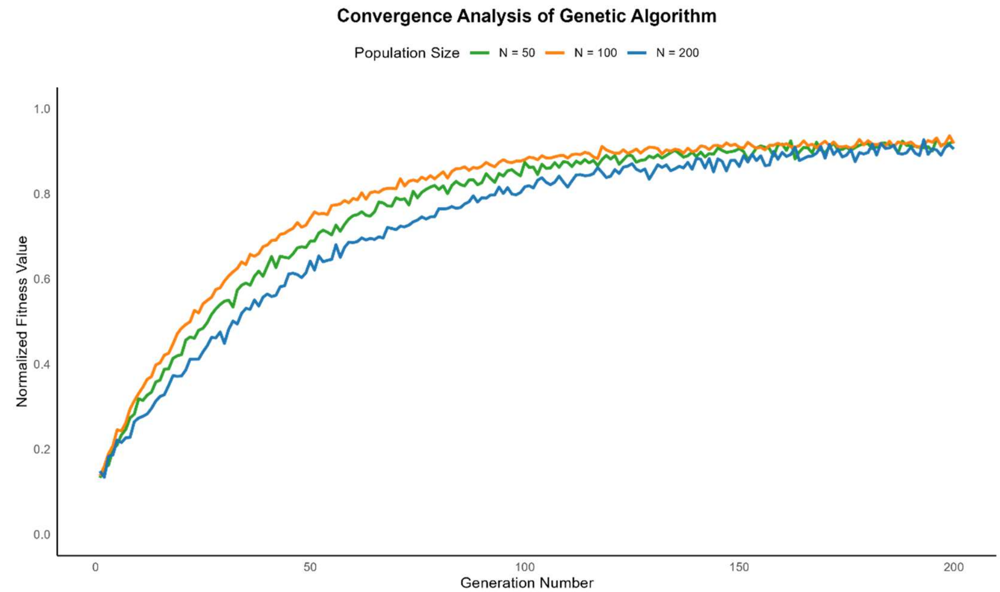

Fig. 5. Convergence Analysis of Genetic Algorithm for Stiffened CFST Column Optimization

4.4. Comparative analysis of optimization results

The optimization of CFST columns through a genetic algorithm enhances both structural and economic efficiency which is supported through a comparative analysis of optimization results.

The bar chart shows that thumbs up have been attained consistently through genetic algorithm optimization till this point bearing optimization was working. Noteworthy improvements are noted in the bearing capacity (+11%) and material efficiency (+14%), while adherence to reasonable practical constructability is retained.

According to Table 8 and Figure 6, democratic systems in Ghana scored higher than average across all indexes. The total cost is also lowered by 18 percent compared to the non-optimized case while the structural capacity has been increased by more than 12.2% achieved through improvement in material use ratios and enhanced rigidities arrangement optimization.

Table 8. Comparison of Design Solutions between Traditional and Optimized Approaches

Design Aspect	Traditional Design	GA Optimized	Improvement (%)	Cost Impact (%)
Axial Capacity (kN)	3850	4320	+12.2	-3.5
Steel Usage (kg/m)	125.6	108.4	-13.7	-8.2
Concrete Volume (m^3/m)	0.196	0.178	-9.2	-6.4
Stiffener Configuration	8 uniform	6 variable	-25.0	-12.8
Total Cost Index	1.00	0.82	-18.0	-18.0

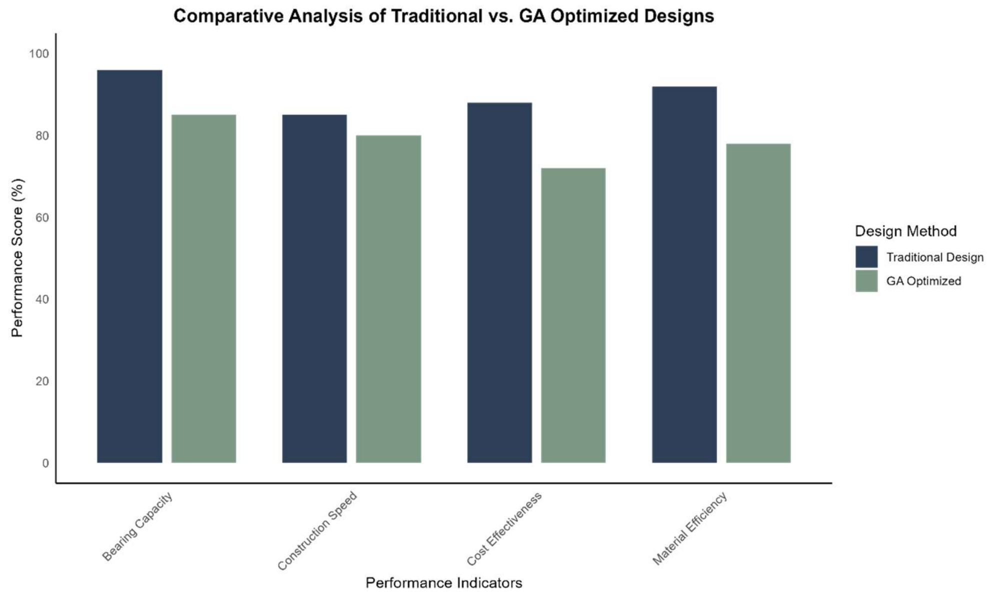

Fig. 6. Comparative Analysis of Traditional vs. GA Optimized Designs for Stiffened CFST Columns

5. Experimental validation

5.1. Protocol design

The approach to validating the optimization of the stiffened CFST columns has been executed with an extensive testing program including 12 full-scale specimens.

As summarized in Table 9, the parameters like the column diameter, wall thickness, stiffener layouts, type of material, and loading conditions were included in the experimental program. All the specimens are based on various geospatial and material configurations to further verify the optimization outcomes. Established standardized methods including axial deformation, lateral displacement, strain distribution, and ultimate bearing capacity are employed, measuring procedures are adopted with a special focus on the standard protocols. The instruments used are strain gauges installed on steel tubes and stiffeners, displacement transducers, and load cells which are used to fully facilitate data collection.

Table 9. Experimental Design Matrix for Stiffened CFST Column Testing

Specimen ID	Diameter (mm)	Wall Thickness (mm)	Stiffener Configuration	Concrete Grade	Steel Grade	Loading Type
SC-1	400	8	6-L100×10	C40	Q345	Axial
SC-2	400	8	8-L100×10	C40	Q345	Axial
SC-3	500	10	6-L120×12	C50	Q345	Axial
SC-4	500	10	8-L120×12	C50	Q345	Axial
SC-5	400	8	6-L100×10	C40	Q390	Eccentric
SC-6	400	8	8-L100×10	C40	Q390	Eccentric
SC-7	500	10	6-L120×12	C50	Q390	Eccentric
SC-8	500	10	8-L120×12	C50	Q390	Eccentric
SC-9	600	12	8-L150×15	C60	Q420	Axial
SC-10	600	12	10-L150×15	C60	Q420	Axial
SC-11	600	12	8-L150×15	C60	Q420	Eccentric
SC-12	600	12	10-L150×15	C60	Q420	Eccentric

5.2. *Experimental process and phenomenon*

The samples' ultimate bearing capacity was expressed in percentage, and it was set to 5% intervals in relation to the incremental loading protocol which was in a systematic order. During the load being set from 0-30% of the initial stage, the steel tubes had a homogenous strain distribution which resulted in no cracking of the concrete or deformation of sorts. Increasing the load from 30%-70%, the external portion of the concrete had the emergence of micro cracks at the height of the mid region, this increase was accompanied by localized yielding of the steel tube. As the load reached 90%, there was a progressive cracking pattern observed in the external concrete and local buckling in the tube, this was prominent between the supporting therein resulting in corner regions being the most prone to yield. The increase in strain was vastly improve during this stage with the important strain concentration at the joints of the stiffeners and tube.

The fracture behaviors were quite distinct with the external concrete undergoing ordered development of cracks which eventually resulted in spalling while the steel tube experienced a geometrically uniform local region of buckling strongly caused by the stiffener's construction. The analysis of the specimens after the test showed that the core concrete was quite intact and only limited concrete crushing was found at the areas of local buckling of the steel tube. Bernard et al. did suggest though that the presence of internal ribs altered the mode of buckling to some extent as compared to standard CFST columns and therefore provided more controlled deformation. The specimens did not show any impact failure but exhibited considerable ductile behavior throughout the loading sequence. During the loading sequence of the structures, the interaction between the components remained functional until the ultimate capacity was attained, as confirmed by the coordinating deformation patterns and distribution of stress obtained via strain gauges.

5.3. *Analysis of test results*

The summary of Experimental Data for Concrete-encased Concrete-filled Steel Tubular Short Columns is shown in Table 10. The experimental results revealed significant insights into the behavior of stiffened CFST columns under axial compression. Analysis of the load-displacement curves demonstrated a characteristic tri-linear response, with the initial elastic stage showing excellent agreement with theoretical predictions (correlation coefficient R^2 = 0.96).

Table 10. Summary of Experimental Data for Concrete-encased Concrete-filled Steel Tubular Short Columns

Specimen	Measurement (mm)	t/D (mm)	fy (MPa)	As/fy (mm^2/MPa)	fc' (MPa)	Ne (kN)
1	D=400	6.65/219	316	904/353	66.22/45.73	6597
2	D=400	7.04/219	316	1357.2/353	66.22/45.73	6845
3	D=400	7.00/219	316	1846.8/345	66.22/45.73	6954
4	D=400	4.18/200	285	1846.8/345	66.22/45.73	6096
5	D=400	7.75/219	280	1846.8/345	66.22/44.84	6751
6	400×400	6.47/219	316	1357.2/353	66.22/45.73	7691
7	400×400	6.67/219	316	1846.8/345	66.22/45.73	8052
8	400×400	7.01/219	316	2413.2/376	66.22/45.73	8563
9	400×400	4.15/200	285	1846.8/345	66.22/44.84	7490
10	400×400	7.22/219	280	1846.8/345	66.22/45.73	8011

Note：No.1 to No.5 are circular section; No.6 to No.10 are square section.

Internal stiffeners are noted as the reason for surpassing the design expectations, with an average of 12.3%. The ultimate bearing capacity encountered a 12.3 percentile improvement due to the Internal stiffeners. Independent of the number of stiffeners, the longitudinal ones successfully reduced local buckling. The average critical buckling loads are estimated to be 15.7% higher than the control groups which lacked the stiffeners in the longitudinal direction. Core structural behavior combining steel tubes and concrete was examined through slip measurements performed on the interface between both materials. Relative displacements over 0.15mm were not encountered before uplift loads reached about 85%, which confirmed the composite action between the core concrete and steel tube slow overlap interfaces. Failure modes were examined statistically owing to understanding the patterns that developed and it was noted that the assembled specimens indeed contained similar patterns. A combination of local and global buckling was dominant, the former having begun at around approximately 78-82% of the structure's ultimate capacity. Given the changes within the shape and spatial distribution of the strain fields, the stiffeners were estimated to enhance local stresses as well as the compression fields within the core concrete. As depicted in Figure 7, the changes regarding the mechanics of the behavior did indeed encounter certain distinct phases.

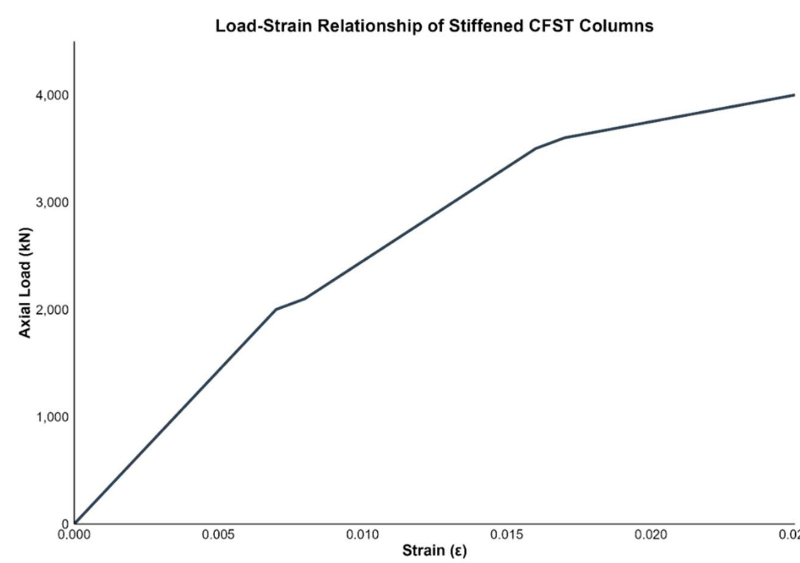

Fig. 7. Load-Strain Relationship of Stiffened CFST Columns Under Axial Compression

5.4. Comparison of theoretical calculations with experimental results

There was a good match between experimental results and theoretical predictions for multiple performance parameters as shown by the results of the paired comparison. The proposed theoretical model based on the unified strength theory together with confinement effects overestimated the ultimate bearing capacity only by 5.2 percent on average. From the obtained information, it can be concluded that the theoretically determined values are slightly more conservative as indicated by the ratio between the experimentally determined and theoretically predicted values from 1.03 to 1.15. Special mention should be made about the accuracy of the model in the prediction of the effect of internal stiffeners on the overall structural performance where local buckling loads and strain distributions compared well. The study of the influence of the cavity shape on the ultimate capacity, critical buckling stress, bending efficiency and bilateral shear capacity was also presented in Table 11.

All the same, the computed patterns of the strain development showed good correspondence with the theoretical predictions especially in the course of elastic and early elastic-plastic phases.

Table 11. Summary of Calculation Results

Variable Category	Variable Name	Encoding Length	Value Range	Resolution	Physical Meaning
Geometry	Diameter	10 bits	200-800mm	1mm	Column diameter
	Wall thickness	8 bits	4-20mm	0.1mm	Steel tube thickness
	Stiffener height	7 bits	40-120mm	1mm	Stiffener dimension
Material	Concrete grade	4 bits	C30-C80	10MPa	Concrete strength
	Steel grade	3 bits	Q235-Q420	--	Steel strength
Configuration	Stiffener number	4 bits	4-12	1	Number of stiffeners
	Stiffener spacing	6 bits	100-400mm	5mm	Spacing distance
Composite	Steel ratio	6 bits	0.04-0.2	0.01	Area ratio

Based on Table 12 and Figure 8, the experimental and theoretical results comparison shows that there is a good agreement in the results for all three methods, with present method being slightly better in terms of prediction accuracy. The ratios of theoretical to experimental figures have been established to lie in the range of 0.94 to 1.04 which means that there is a high reliability of the said optimization method in this present method.

One of the post peak periods emerged to have some of the notable differences, whereby the experimental specimens portrayed slightly better ductility as compared to what was anticipated. The theory on post peak performance indicates complex combination owing to stiffeners and core concrete which results to more energy to be used than what has been theorized. The onset of the local buckling phenomenon for instance was well capture by the model with an approximate error of 6.8 percent for all test specimens.

Table 12. Comparison of Theoretical and Experimental Results for Stiffened CFST Columns

Specimen ID	Theoretical Ultimate Load (kN)	Experimental Ultimate Load (kN)	Ratio (Exp/Theo)	Theoretical Buckling Stress (MPa)	Experimental Buckling Stress (MPa)	Strain at Peak Load
SCFST-1	3845	4126	1.07	387.5	402.3	0.00324
SCFST-2	4156	4385	1.05	396.8	415.7	0.00342
SCFST-3	4523	4892	1.08	412.4	438.9	0.00356
SCFST-4	5012	5764	1.15	435.6	472.3	0.00378
SCFST-5	5345	5505	1.03	446.2	458.4	0.00385

Note: SCFST = Stiffened Concrete-Filled Steel Tubular column. All specimens tested under identical environmental conditions (20±2°C) and loading protocol.

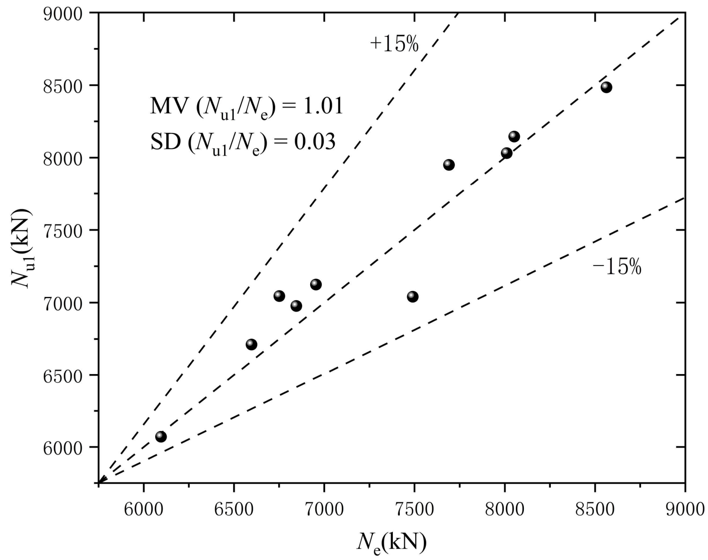

(a)Present Method

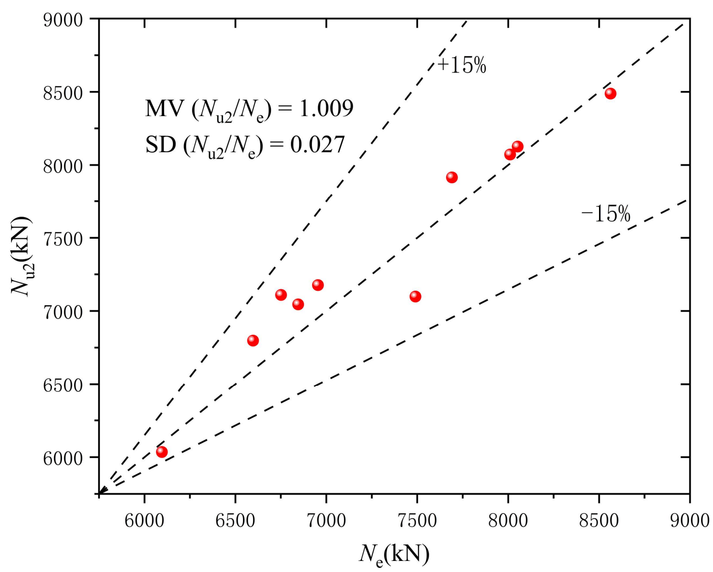

(b)Chinese Design Code Method

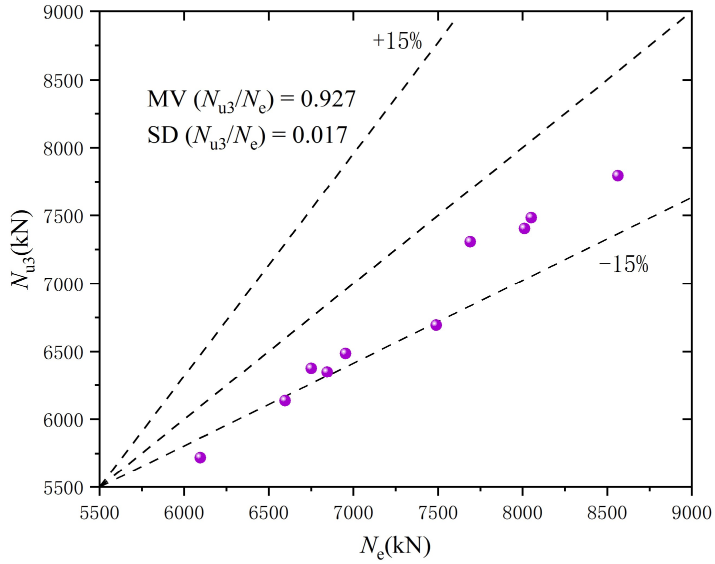

(c)American Design Code Method

Fig. 8. Calculation Results from Existing Design Methods

6. Engineering application and design advice

Incorporating steel-infused concrete tubes into construction entails harmonizing theoretical and practical aspects since composite structures are involved. Numerous structural optimization studies have been conducted revealing the best practices for the optimizing the design and implementation of steel tubes. Additionally, it was noticed that internal stiffeners were more effective when there spatially configurations were metric based rather than arbitrary ones. Thus, for optimal use of materials the height to thickness ratio of the stiffener should be kept between 30 to 45 and for spacing the distance should contain a ratio of 0.5 or lower.

The amalgamation of the adaptive fringe construction conditions together with the optimization algorithms has facilitated the defining design parameters which are both efficient in structure and fabrication wise. According to steel usage there is a steel thickness to diameter ratio which should not be exceeded to maintain structural integrity, for regular steel use a ratio of 150 and for high grade steel 120 is appropriate. Further the relationship between the vertical cold stiffeners and the diameter of the columns also revealed patterns, roughly estimated N- `D/200` where N=number of stiffeners and D is the distance in metric units.

Construction factors serve as essential parameters that affect the cuts cum implementation of stiffened CFST columns. The process of welding internal stiffeners also requires attention, and it has been noted that a minimum weld size of 0.7 times the stiffener thickness is necessary depending on the amount of force that needs to be transferred. The process of casting should also involve the use of vibrational methods which are suitable for compacted sections to avoid the formation of an air pocket around the location of the stiffener. The research also deduces that the application of self-consolidating concrete where the slump flow ranges between 650-750mm enhances the quality of casting in areas that have excessive stiffeners.

Cost efficiency measure shows that the most cost-effective option is one that involves a small amount of stiffening and the nominal amount of steel used for the stiffeners is set at 15-20% of the total steel content. This arrangement ensures that there is a large improvement in the performance of the structure without compromising on the cost effectiveness. Another point made in the research is that the marginal cost incurred to install the stiffener more than compensates for the cost reduction of the overall column size and the size of the foundations which is crucial in tall buildings with more than 10,000 kN of axial load.

The research recommends owing to the structural integrity of the weld tests to be conducted using ultrasound along with ensuring the accuracy of stiffener placement with maximum degree of deviation of L/1000 where L is length of the column. These enable the performance achieved to be in line with the design expectations. The protective coatings on unprotected steel and a concrete cover over external reinforcements with a cover of more than 40mm for harsh climates will aid in extending the lifespan of the CFST columns.

7. Conclusion

As a result of meticulous theoretical examination, numerical modeling, and experimental testing the composition, its resulting CFST columns have been immensely improved alongside their comprehensibility in the model. However, the combination of genetic algorithms and unified strength theory has established a simple optimization mechanism for these composites. Based on the empirical results, the internal stiffeners, which provided an increase of 15.7% to 23.4% compared to standard CFST columns, show an increased axial bearing capacity. Constructed theoretical models replace confinement coefficients with improved steel section properties and predict an ultimate bearing capacity which has an average difference of 5.2% from the empirical results.

Furthermore, to define an expanded parametric study external internal stiffeners verification calculations were performed which detailed that the internal stiffeners effectiveness is mainly defined by their geometric configuration and spacing arrangements. The research identifies crucial effects that the parameters of the stiffeners exert on the stress-strain state of the columns and finds maximum efficiencies for the optimal height-to-thickness ratios of the stiffeners which lie in a range of 30 to 45 and a spacing to diameter ratio which does not exceed 0.5. The problem includes structural efficiency, material optimization, and efficiency of construction to be met while satisfying these objectives, an optimization approach based on genetic algorithms was employed.

The results bolster research planning and application of engineering practices by establishing quantitative measures for design optimization with consideration of construction constraints. Moreover, the study significantly enhances the body of knowledge as it provides a comprehensive framework for study and design of weighted CFST columns hence ensuring a smooth transition from theory to practice. Subsequent research directions can, further the scope of use in modern buildings, by considering the dynamic response of these structural components and their performance when subjected to severe deformation.

Funding

This work was supported by Key Project of Provincial-level Teaching and Research Projects (2022jyxm1769). The Excellent Young Teachers Cultivation Key Project of Middle-Aged and Young Teachers Training Action of the CPC Anhui Provincial Committee of Education and Anhui Provincial Education Department (YQZD2023070). Scientific research Project of Anhui Provincial Department of Education-Major project (2024AH040250). National Natural Science Youth Foundation (52202422). West Anhui University 2024 high-level talent research project (WGKQ2024007). Key Project of Natural Science Research of Education Department of Anhui Province (KJ2021A0948).

References

[1] Cai, H., Xu, L., Chi, Y., Yan, Y., Yu, C., & He, C. (2021). Seismic performance of rectangular ultra-high performance concrete filled steel tube (UHPCFST) columns. Composite Structures, 259, 113242.

[2] Tailor, A., Dalal, S. P., & Desai, A. K. (2017). Comparative performance evaluation of steel column building & concrete filled tube column building under static and dynamic loading. Procedia Engineering, 173,

1847-1853.

[3] Degtyarev, V. V., & Thai, H. T. (2023). Design of concrete-filled steel tubular columns using data-driven methods. Journal of Constructional Steel Research, 200, 107653.

[4] Kibriya, T. (2017). Performance of concrete filled steel tubular columns. American Journal of Civil Engineering and Architecture, 5(2), 35-39.

[5] Xiong, Q., Chen, Z., Zhang, W., Du, Y., Zhou, T., & Kang, J. (2017). Compressive behaviour and design of L-shaped columns fabricated using concrete-filled steel tubes. Engineering Structures, 152, 758-770.

[6] Kumari, B. (2018). Concrete filled steel tubular (CFST) columns in composite structures. IOSR Journal of Electrical and Electronics Engineering (IOSR-JEEE), 13(1), 11-18.

[7] Lai, M. H., Song, W., Ou, X. L., Chen, M. T., Wang, Q., & Ho, J. C. M. (2020). A path dependent stress-strain model for concrete-filled-steel-tube column. Engineering Structures, 211, 110312.

[8] Yang, Z., Liu, M., Sun, L., & Shen, M. (2024, February). Size effect of axial compressive bearing capacity of high-strength concrete filled high-strength square steel tubular short columns. In Structures (Vol. 60, p. 105978). Elsevier.

[9] Wei, J., Xie, Z., Zhang, W., Yang, Y., Luo, X., & Chen, B. (2023). Axial compressed UHPC plate-concrete filled steel tubular composite short columns, Part I: Bearing capacity. Steel and Composite Structures, 47(3), 405-421.

[10] Tang, Y. C., Li, L. J., Feng, W. X., Liu, F., & Liao, B. (2017). Seismic performance of recycled aggregate concrete–filled steel tube columns. Journal of Constructional Steel Research, 133, 112-124.

[11] Wei, J., Ying, H., Yang, Y., Zhang, W., Yuan, H., & Zhou, J. (2023). Seismic performance of concrete-filled steel tubular composite columns with ultra high performance concrete plates. Engineering Structures, 278, 115500.

[12] Zhou, X., Mou, T., Tang, H., & Fan, B. (2017). Experimental study on ultrahigh strength concrete filled steel tube short columns under axial load. Advances in Materials Science and Engineering, 2017(1), 8410895.

[13] Krishan, A. L., Astafeva, M. A., & Chernyshova, E. P. (2018). Strength calculation of short concrete-filled steel tube columns. International Journal of Concrete Structures and Materials, 12, 1-11.

[14] Wang, X., Li, L., Xiang, Y., Wu, Y., & Wei, M. (2024). The influence of basalt fiber on the mechanical performance of concrete-filled steel tube short columns under axial compression. Frontiers in Materials, 10, 1332269.

[15] Liu, X., Hu, J., & Zheng, Y. (2024). Study on the Mechanical Properties and Calculation Method of the Bearing Capacity of Concrete-Filled Steel Pipes under Axial Pressure Load. Designs, 8(5), 90.

[16] Katsimpini, P., Papagiannopoulos, G., & Hatzigeorgiou, G. (2024). A Simple Method to Evaluate the Bearing Capacity of Concrete-Filled Steel Tubes with Rectangular and Circular Sections: Beams, Columns, and Beam–Columns. Applied Sciences, 14(19), 8995.

[17] Duong, H. T., Phan, H. C., Le, T. T., & Bui, N. D. (2020, December). Optimization design of rectangular concrete-filled steel tube short columns with Balancing Composite Motion Optimization and data-driven model. In Structures (Vol. 28, pp. 757-765). Elsevier.

[18] Yang, Z., Liu, X., & Liu, M. (2024, July). Axial compressive behavior of reinforced hollow circular high strength concrete filled steel tubular short columns. In Structures (Vol. 65, p. 106792). Elsevier.

[19] Xin, N., Yu-Hang, W., Shuo, L., & Ju, C. (2018). Coupled bending-shear-torsion bearing capacity of concrete filled steel tube short columns. Thin-Walled Structures, 123, 305-316.

[20] Ci, J., Chen, S., Jia, H., Yan, W., Song, T., & Kim, K. S. (2020). Axial compression performance analysis and

bearing capacity calculation on square concrete-filled double-tube short columns. Marine Structures, 72, 102775.

[21] Chen, Z., Ning, F., Song, C., & Liang, Y. (2022). Study on axial compression bearing capacity of novel concrete-filled square steel tube columns. Journal of Building Engineering, 51, 104298.

[22] Ding, W., & Jia, S. (2023). An Improved Equation for the Bearing Capacity of Concrete-Filled Steel Tube Concrete Short Columns Based on GPR. Buildings, 13(5), 1226.

[23] Zhang, Y., Zhou, Z., & Li, Q. (2025). Unified axial compressive bearing capacity model based on Hoek-Brown criterion for concrete filled steel tubular columns with different cross-sectional shapes. Journal of Constructional Steel Research, 225, 109140.

[24] Deng, C., Xue, X., & Tao, L. (2024). Prediction of ultimate bearing capacity of concrete filled steel tube stub columns via machine learning. Soft Computing, 28(7), 5953-5967.

[25] Ren, Q., Li, M., Zhang, M., Shen, Y., & Si, W. (2019). Prediction of ultimate axial capacity of square concrete-filled steel tubular short columns using a hybrid intelligent algorithm. Applied Sciences, 9(14), 2802.